

# Synthesis of Microporous Cobalt Silicate using Organic Template Derived from 2,6-Dimethylpiperidinium Cations: A Potential Precursor for the Preparation of Double Perovskite Cobalt Materials

Davi Rubinho Ratero<sup>1</sup>, Erick Paiva Cancelli<sup>1</sup> and José Geraldo Nery<sup>1,\*</sup>

<sup>1</sup>Physics Department, IBILCE, São Paulo State University- UNESP, São José do Rio Preto Campus, São Paulo 15054-000, Brazil

**Abstract:** Synthesis of a microporous cobalt silicate was achieved by using 6,10-dimethyl-5-azoniaspiro[4, 5] decane bromide as structure directing agent. And physicochemical characterization was carried out using XRD, SEM, HTEM, TGA, FT-IR, BET-N<sub>2</sub>, ICP-OES and EDS. ETS-10 like structure framework was present as a competitive phase. Calcination of the cobalt silicate at 500 °C leads to a new structure. The possibility of this material be cobalt oxide was excluded since Bragg reflections at  $2\theta = 19.2^\circ$ ;  $30.3^\circ$ ;  $36.9^\circ$ ;  $43.7^\circ$ ;  $59.2^\circ$  were absent (JCPDS#80-1538). Both the indexation of the XRD data for the calcined material which has resulted in a tetragonal unit cell ( $a = b = 10.39 \text{ \AA}$  and  $c = 12.21 \text{ \AA}$ ,  $\alpha = \beta = \gamma = 90^\circ$ ,  $V = 1317.4 \text{ \AA}^3$ ) and HTEM data indicated the cobalt silicate can be used as a precursor for the preparation of double perovskite cobalt materials.

**Keywords:** Organic template, Cobalt silicate, Double perovskite cobalt.

## 1. INTRODUCTION

Zeolites are crystalline microporous materials based on aluminosilicates with well-defined pore structures built of  $[\text{SiO}_4]^{4-}$  and  $[\text{AlO}_4]^{5-}$  tetrahedra with diameters smaller than 10 Å and containing active sites that can be generated in the zeolite framework [1]. Depending on zeolite chemical composition, different pore sizes, acidity, basicity, thermal resistance, and ion exchange selectivity, different specificities of the active catalytic sites can be formed. These properties have direct dependence on the conditions of the synthesis and the way that it is performed. Zeolites are usually synthesized by hydrothermal sol-gel reactions, under specific conditions of temperature, pressure and controlled pH to fine-tune the final zeolites properties. The possibility of tailoring the strength and concentration of the active basic or acidic sites, surface area, and adsorption properties of zeolitic materials make them attractive heterogeneous catalysts to produce petrochemicals, detergents builders, sensors, and adsorbents for environmental remediation [2-5].

Substitution of Si or Al atoms in the crystallographic zeolite structure by transition atoms such as Ti, V, Zr, Ge, Sn, Nb, Y, Cr, Co and Mo favours the formation of zeolites with different physicochemical properties and new topologies of pores, channels, and cavities [6].

Zeolites containing silicon atoms with tetrahedral geometry and transition metal atoms with octahedral or pentahedral geometry in their crystallographic networks are defined as microporous materials of mixed structures or OPT materials. The monomeric units that form these inorganic polymers are made of silicon tetrahedrons ( $\text{SiO}_4$ ) and the octahedrons ( $\text{MO}_6$ ) or pentahedrons ( $\text{MO}_5$ ) of transition metals. The first works related to the synthesis and characterization of mixed-structure microporous (OPT) materials, including cobalt-silicate based materials date back to the late 1980's and early 1990's [7-10].

Materials with zeolitic structure based on cobalt silicates have been studied since the 80's due to their catalytic properties [11-13]. Among applications in catalysis, the reduction of  $\text{NO}_x$  [14]; Fischer-Tropsch reactions [15]; oxidation of aromatic compounds [16], and hydrogenation reactions [17]. There are several methods for synthesis of zeolitic materials containing cobalt, either integrated into the structure, or impregnated on the surface, or even adsorbed under the ion exchange process [18]. In general, hydrothermal syntheses are used in a reaction medium containing cobalt salts and a silica source, in an acidic or basic aqueous medium, with temperatures in the range of 100-200 °C. The patent literature presents examples of application of cobalt-based crystalline materials as molecular sieves [19-21] and as catalysts, for example, in hydrocarbon conversion reactions [22] and reduction of nitrogen oxides [23].

\*Address correspondence to this author at the Physics Department, IBILCE, UNESP – São Paulo State University, São José do Rio Preto Campus, São Paulo 15054-000, Brazil; Tel: +55 17 3221 2490; Fax: +55 17 3221 2247; E-mail: geraldo.nery@unesp.br

This paper reports the sol-gel synthesis and the physicochemical characterization performed by XRD, SEM, EDS, HTEM, TGA, BET, FT-IR, and ICP-OES of a new cobalt silicate and the discussion of its possible applications.

## 2. MATERIALS AND METHODS

Ludox HS-30 (27% m/m SiO<sub>2</sub>); NaOH; KF, CoSO<sub>4</sub>·7 H<sub>2</sub>O; 2,6-dimethylpiperidine (mixture of isomers) were purchased from Sigma-Aldrich and used without further purification. Inorganic salts and organic bases used for the preparation of zeolitic matrices were of reagent grade (≥ 98%).

### 2.1. Synthesis of SDA 6,10-Dimethyl-5-Azoniaspiro [4.5] Decane

Synthesis of 6,10-dimethyl-5-azoniaspiro[4.5] decane bromide SDA is schematized in Figure 1. A typical synthesis is prepared as follows: one mole of cis-2,6-dimethyl-piperidine is consumed in 170 mL of methanol along with 2 moles of potassium bicarbonate (KHCO<sub>3</sub>). Then, one mole of 1,4-dibromopentane is added to this system, drop by drop. The reaction mixture is then maintained under stirring and reflux for

72 hours. Afterwards, the mixture is cooled, and methanol is evaporated in a system coupled to a heating bath and a vacuum pump. At the end of the process, the solid phase is extracted with chloroform.

### 2.2. Synthesis of Cobalt Silicate

Cobalt silicate synthesis consists of three parts, as illustrated in Figure 2. First, a solution was prepared following the order of addition of the components, under constant stirring: 8.49 g of H<sub>2</sub>O; 1.86 g of Ludox HS-30, then 1.05 g of 6,10-dimethyl-5-azoniaspiro [4.5] decane bromide; after the structure director, 0.21 g of NaOH was added and finally, after complete dissolution, 0.57 g of KF. The second step consisted of preparing a solution containing 1.23 g of H<sub>2</sub>O and 0.55 g of CoSO<sub>4</sub>·7 H<sub>2</sub>O; this solution presented a strong red colour. The Co solution was then mixed into the first solution and immediately the colour of the mixture turned blue-purple, and a homogeneous gel started to form. This mixture was kept under constant stirring for another hour and the pH of the gel was measured at 13.0. The last step of the synthesis was to place the gel in a hydrothermal reactor and take it to the oven for 7 days at 180 °C. After one week, the reactor contained

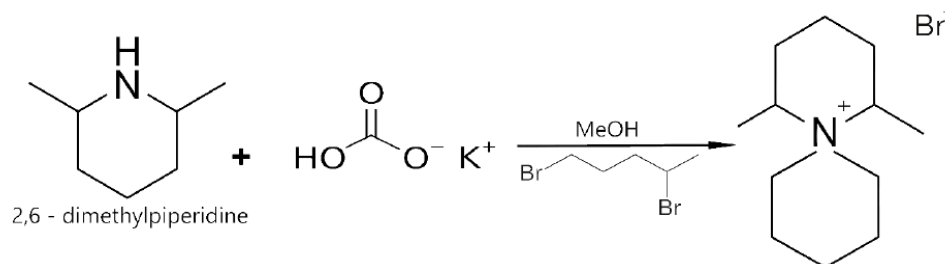


**Figure 1:** Schematic synthesis for preparation of structure directing agent derivative from 2,6-dimethylpiperidinium cations.

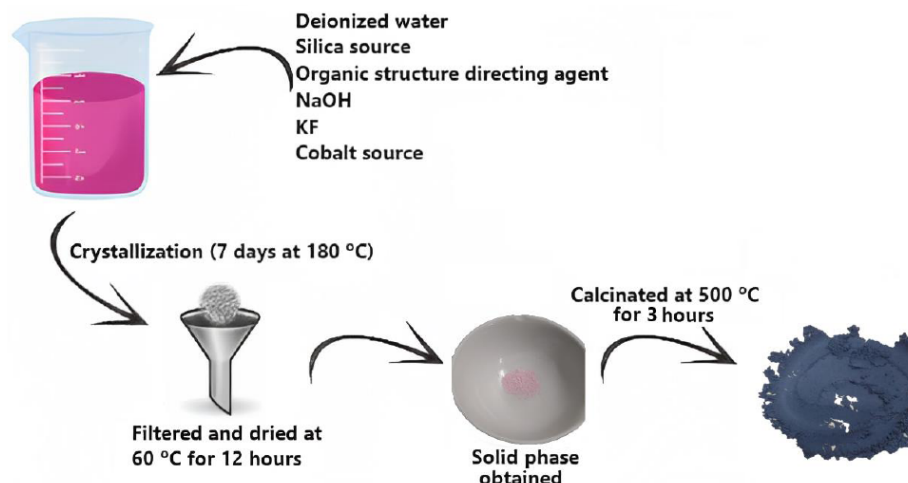


**Figure 2:** Schematic illustration for preparation of sol-gel cobalt silicate.

two phases, one solid and one liquid. The solid phase was separated by filtration and washed with deionized water, then placed to dry in an oven at 60 °C for 12 hours. The resulting solid has a pinkish colour.

After synthesis, the cobalt silicate material is still impregnated with the 6,10-dimethyl-5-azoniaspiro [4.5] decane bromide. In order to remove the organic molecule, a thermal treatment was performed consisting of calcination in a muffle furnace, following a temperature ramp: 30 min from 25-100 °C; 30 min from 100-200 °C; 30 min from 200 to 300 °C, then 30 min from 300-400 °C and 30 min from 400-500 °C. The sample was then kept for another 3 hours at 500 °C and then cooled naturally to room temperature. The calcined material is a dark blue one.

### 2.3. Physicochemical Characterization

Physicochemical characterization of cobalt silicate was performed using X-ray Powder diffraction (XRD), Scanning electron microscopy (SEM); Energy dispersive spectroscopy (EDS), High resolution electron transmission microscopy (HTEM); Fourier transform-infrared spectroscopy (FT-IR); BET-N<sub>2</sub> adsorption Thermogravimetric analysis (TGA). Elemental chemical analysis was performed by Optical emission spectroscopy with coupled plasma (ICP-OES). XRD analyses were performed in a Rigaku Miniflex II diffractometer operating at 30 kV and 15 mA, using a nickel filter and radiation CuK $\alpha$  ( $\lambda = 1.5418 \text{ \AA}$ ). The diffraction patterns were obtained using a  $2\theta$  range from 3° to 80° with the goniometer at a rate of 2° ( $2\theta$ ) min<sup>-1</sup>. Scanning electron microscopy (SEM) images were recorded at the Brazilian National Nanotechnology Laboratory (National Center for Energy and Materials Research), in Campinas (São Paulo State), using a Phillips XL30 FEG instrument operating with electron beam voltages from 5 to 25 kV. Additional analyses were performed at LCE-DEMA (UFSCar, São Carlos, São Paulo State), using an FEI Inspect S50 scanning electron microscope operated with an electron beam voltage of 25 kV.

FT-IR analyses were performed in a Shimadzu IRTracer-100 Spectrometer; samples were analysed with 32 scans with a resolution capacity of 2 cm<sup>-1</sup> between wavelengths of 400 cm<sup>-1</sup> to 4000 cm<sup>-1</sup> using the KBr pellet technique. Elemental chemical analysis for Si, Co, Na, and K, was determined by Inductively Coupled Plasma-Optical Emission Spectroscopy using an Arcos model ICP-OES Spectrometer, with sample digestion done by fluorination and alkaline fusion with

lithium tetraborate, followed by dissolution with nitric acid, using approximately 75 mg of material for each sample. TGA analysis carried out on a Netzsch 429 instrument. The as made synthesized samples (5 mg) were heated in a stream of synthetic air (50 mL/min with a heating rate of 10 °C/min in the temperature range 25-1000 °C). BET-N<sub>2</sub> analysis were performed at -196 °C in a Micromeritics adsorption analyser model ASAP 2020; for this, approximately 0.2 g of sample was submitted to a gas flow at 150 °C for 24 h and then analysed by the BET method.

### 3. RESULTS AND DISCUSSION

XRD data for the as made and calcined cobalt silicate sample are shown in Figure 3, The XRD pattern of the as made cobalt silicate shows diffraction peaks located  $2\theta = 6.17^\circ; 11.09^\circ; 21.02^\circ; 23.35^\circ; 26.94^\circ; 30.27^\circ; 31.45^\circ; 38.53^\circ; 47.71^\circ$  and  $56.05^\circ$ . A careful analysis of XRD patterns clearly indicates that the cobalt silicate is not a pure phase material and there are other competitive phases. One of the competitive phases could be assigned to the ETS-10 titanosilicate [24,25]. ETS-10 which is characterized by two broad diffraction peaks at  $2\theta = 6.17$  and  $11.09^\circ$ . A literature survey concerning the ETS-10 synthesis in the absence or presence of organic templates revealed that the most common competitive or impurity phases were ETS-4, AM-1, AM-2, AM-3, and/or AM-4 [26]. Paula and co-workers have intensively studied the sol-gel chemistry of titanosilicate ETS-10 in the presence of 2,6-dimethylpiperidinium cations and decahydroquinolium, piperidinium and (S)-Spartenium cations and high crystalline ETS-10 were obtained, however the competitive phase previously reported were not detected when using 2,6-dimethylpiperidinium cations [27-30]. After calcination, Bragg diffraction peaks located at  $2\theta = 6.17^\circ; 11.09^\circ; 21.02^\circ; 30.27^\circ; 31.45^\circ$  disappeared (Figure 3) and the possibility of cobalt oxide formation excluded since the ( $2\theta = 19.2^\circ; 30.3^\circ; 36.9^\circ; 43.7^\circ; 59.2^\circ$ ) were absent (JCPDS#80-1538). A tetragonal unit cell ( $a = b = 10.39 \text{ \AA}$  and  $c = 12.21 \text{ \AA}$ ,  $\alpha = \beta = \gamma = 90^\circ$ ,  $V = 1317.4 \text{ \AA}^3$ ) were obtained using TREOR [31]. Howe *et al.*, have discussed the incorporation of cobalt cations into the ETS-10 framework. In their work the incorporation of cobalt species was achieved without organic templates and the final cobalt content was around (1.5%) [32], while by using 6,10-dimethyl-5-azoniaspiro [4.5] decane bromide an incorporation of 15.4 % was achieved in this current research according to the ICP-OES analysis (Si = 16.30%; Co = 15.40%; Na = 8.24%; K = 5.60%).

Oxide catalysts that are both active and stable for the oxygen evolution reaction upon water oxidation in alkaline solution have been extensively reported in the literature and double perovskites are very suitable oxide catalysts for this purpose [33-35]. The unit cell parameters found for the cobalt silicate in this study are larger than the  $\text{PrBaCo}_2\text{O}_{5.75}$  ( $a = b = 3.9005(8) \text{ \AA}$ ,  $c = 7.6389(1) \text{ \AA}$ ,  $V = 116.217(5) \text{ \AA}^3$ , space group  $P4/mmm$ ) and  $\text{PrBaCo}_2\text{O}_{5.5}$  ( $a = 3.9066(8) \text{ \AA}$ ,  $b = 7.8737(5) \text{ \AA}$ ,  $c = 7.6049(4) \text{ \AA}$ ,  $V = 233.922(1) \text{ \AA}^3$ , space group  $P4/mmm$ ) reported by Miao *et al* [35] and these preliminary data can suggest that this cobalt silicate can be possibly used as precursor for cobalt perovskite formation. Although the formation of ceramic phase from zeolite have been reported since the seminal work of Breck *et al.*, [36] the advantages of using zeolite as precursors for the preparation of aluminosilicate ceramics were extensively reported by several authors [37] the possibility of microporous cobalt silicate as a precursors for the synthesis of for cobalt perovskite arises as a viable possibility as suggested by the experimental data herein reported.

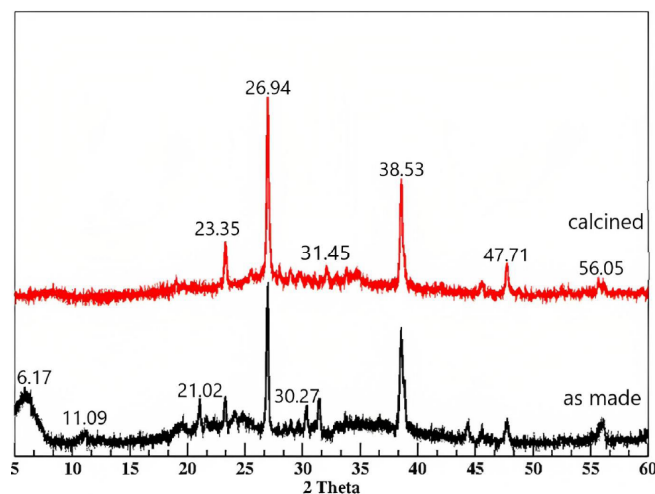


**Figure 3:** Powder XRD patterns of cobalt silicates synthesized with organic template derived from 2,6-dimethylpiperidinium cations.

Figure 4 shows the SEM and HTEM of the cobalt silicate. SEM images reveal that the morphology of this cobalt silicate can be described as a tangle of line-like structures which resemble a coral structure with pores and cavities. Further evidence of the double perovskite

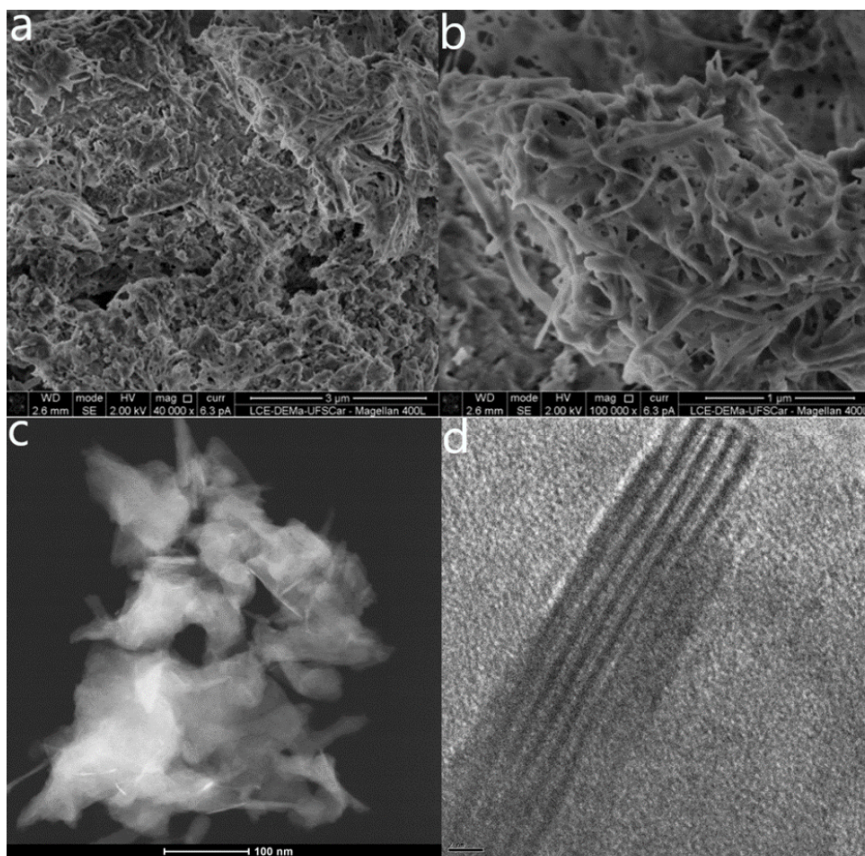


**Figure 4:** SEM and HTEM images of cobalt silicate material with different magnifications: a) 40000x; b) 100000x c) High resolution transmission electron micrograph images for cobalt silicate, with scaling of 100 nm. d) High resolution transmission electron micrograph images for cobalt silicate with scaling of 2nm.

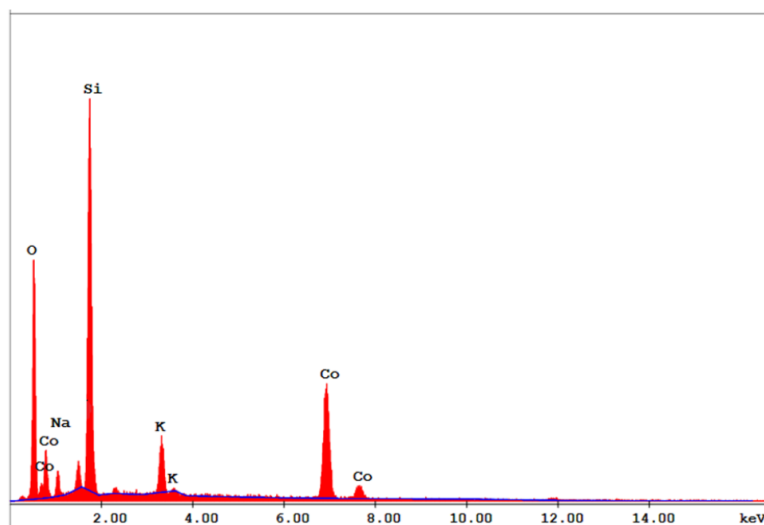
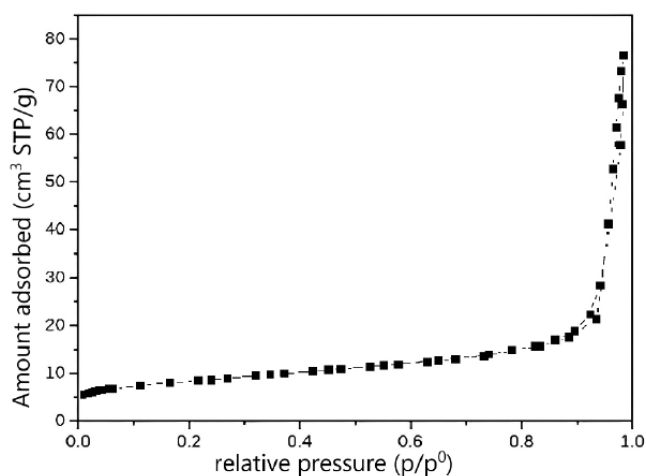


**Figure 5:** EDS spectrum of cobalt silicate material.

cobalt is provided by TEM images. A comparison of the HTEM showed in Figure 4d with the data reported by Horn *et al.*, [38].

Figure 5 shows the EDS data, and the chemical composition is in accordance with the pristine sol-gel chemistry composition. It is worth to mention that no signs of the carbon due to the use of SDAs were found in the EDS spectrum. Atomic percentage of Si (23.7%), Co (9.9%) which gives a Si/Co ratio of approximately 2.4 is in accordance with the amounts determined by ICP-OES analysis (Si = 16.30%; Co = 15.40%; Na = 8.24%; and K = 5.60%).

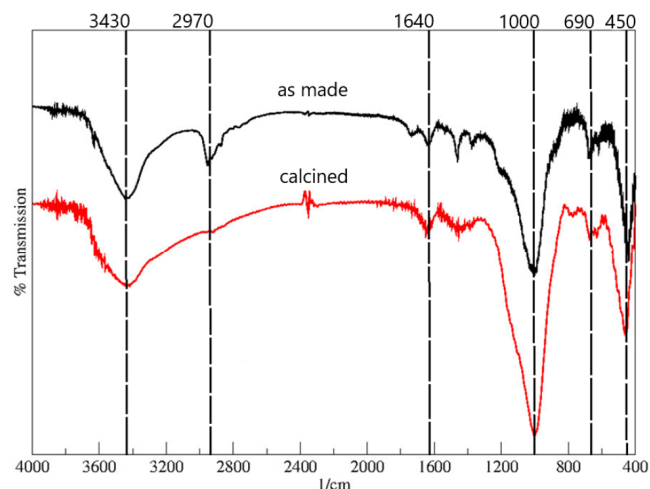
The data for surface area analysis of this material is shown in Figure 6. Surface area calculated by the BET method was  $27.9 \text{ m}^2\text{g}^{-1}$ , and the total and pore volume  $0.1184 \text{ cm}^3\text{g}^{-1}$



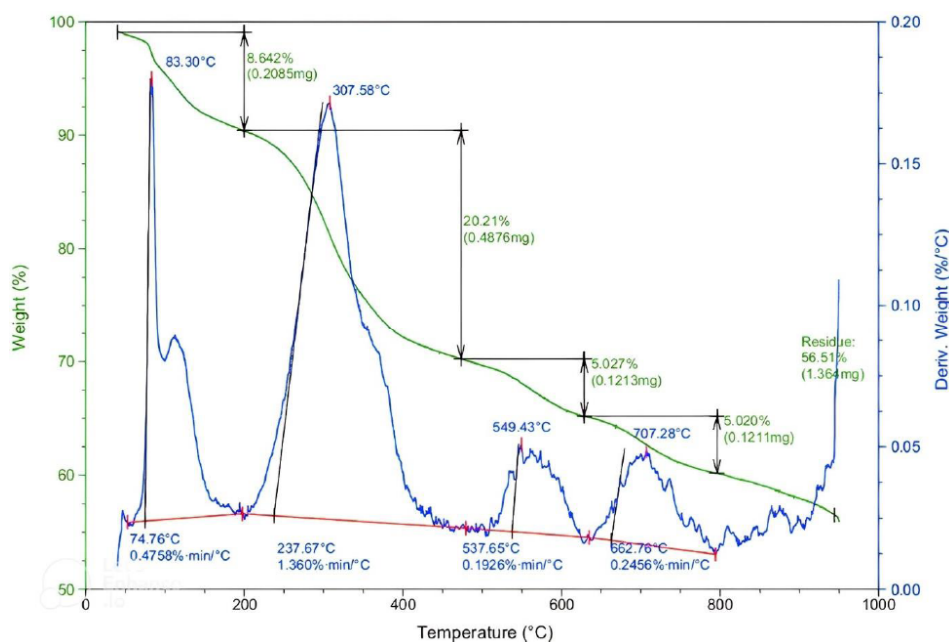
**Figure 6:** Nitrogen adsorption-desorption isotherm for cobalt silicate after heat treatment.

Figure 7 shows the FT-IR data for both the as made and calcined cobalt silicate. Results show that there was a band ( $2800\text{-}3000 \text{ cm}^{-1}$ ) associated with the presence of amine groups from the SDA and it was removed after the calcination treatment. The band located at  $3400 \text{ cm}^{-1}$  is associated with O-H groups which are determined to water molecules at the cobalt silicate (as made sample) and to the silanol groups (calcined sample) [38]. The absorption bands located between  $1400\text{-}1800 \text{ cm}^{-1}$  are associated with the stretching of the C-C bonds of the organic SDA. A decrease in the intensity of these bands can be noticed before and after calcination treatment.

The absorption bands located in the  $1000\text{-}450 \text{ cm}^{-1}$  corresponds to the asymmetric stretching of the Si-O bonds of the  $\text{SiO}_4$  tetrahedral.



**Figure 7:** FT-IR transmission spectrum of cobalt silicate material; the black line shows the material before heat treatment to remove SDA; the red line is the material in its final stage.



**Figure 8:** Typical TGA curves for the as made cobalt silicates.

TGA curves for the material are presented in Figure 8. As the temperature increases, cobalt silicate undergoes four major mass losses, the first in the range of 83-200 °C, in which there is the loss of water molecules from the external part of the crystalline structure of the material. Then, from 300-530 °C there is a loss of 20.21% in mass, due to the complete loss of the organic molecules of the structure director; followed by two more mass losses, at 650 °C and 800 °C, associated with the loss of structural water, followed by the collapse of the structure at approximately 900 °C. This behaviour evidence that the process for removing the organic structure directing agent at 500 °C is effective, by doing it without damaging the crystalline structure of the solid; moreover, these results show that cobalt silicate presents a structure capable of withstanding elevated temperatures, of the order of 700 °C without collapsing.

#### 4. CONCLUSIONS

Cobalt silicate was successfully synthesized using 6,10-dimethyl-5-azoniaspiro [4.5] decane bromide as structure directing agent. ETS-10 framework material was detected as a competitive phase. Calcination of the cobalt silicate at 500°C results in a material with a cobalt perovskite like structure as indicated by XRD and HTEM data. The findings open the possibility of using microporous cobalt silicate as a precursor for the synthesis of double perovskite cobalt.

#### DECLARATION OF COMPETING INTEREST

The authors declare that they have no known competing financial interests or personal relationships that could have appeared to influence the work reported in this paper.

#### CREDIT AUTHORSHIP CONTRIBUTION STATEMENT

**Davi Rubinho Ratero:** Investigation, data curation, writing – original draft.; **Erick Paiva Cancellari:** investigation, data acquisition and writing. **José Geraldo Nery:** Funding acquisition, project administration, supervision, conceptualization, writing – review & editing.

#### ACKNOWLEDGMENTS

This work has been supported by The State of São Paulo Research Foundation (FAPESP) in the form of a scientific award to J.G.N (2019/01858-5). We also would like to thank CAPES for financial support under Award #406761/2013-2 and 88887.513909/2020-00.

#### REFERENCES

- [1] Cundy, C. S.; Cox, P. A. The hydrothermal synthesis of zeolites: History and development from the earliest days to the present time. *Chemical Reviews*, v. 103, n. 3, p. 663-701, Mar 2003. <https://doi.org/10.1021/cr020060j>
- [2] C.S. Cundy, P.A. Cox, The hydrothermal synthesis of zeolites: precursors, intermediates and reaction mechanism,

- Microporous Mesoporous Mater. 82 (2005) 1-78.  
<https://doi.org/10.1016/j.micromeso.2005.02.016>
- [3] M. Panayotova, B. Velikov, Kinetics of heavy metal ions removal by use of Natural Zeolite, *J. Environ. Sci. Health, Part A*. 37 (2002) 139-147.  
<https://doi.org/10.1081/ESE-120002578>
- [4] M. Delkash, B. Ebrazi Bakhshayesh, H. Kazemian, Using zeolitic adsorbents to clean up special wastewater streams: a review, *Microporous Mesoporous Mater.* 214 (2015) 224-241.  
<https://doi.org/10.1016/j.micromeso.2015.04.039>
- [5] J. Rocha, M.W. Anderson, Microporous titanosilicates and other novel mixed octahedral-tetrahedral framework oxides, *Eur. J. Inorg. Chem.* 18 (2000).  
[https://doi.org/10.1002/\(SICI\)1099-0682\(200005\)2000:5<801::AID-EJIC801>3.0.CO;2-E](https://doi.org/10.1002/(SICI)1099-0682(200005)2000:5<801::AID-EJIC801>3.0.CO;2-E)
- [6] J. Rocha, P. Ferreira, Z. Lin, P. Brandão, A. Ferreira, J.D. Pedrosa de Jesus, Synthesis and structural characterization of microporous yttrium and calcium silicates, *J. Phys. Chem. B* 102 (1998).  
<https://doi.org/10.1021/jp9803337>
- [7] KUZNICKI, S. M. New crystalline titanium silicate molecular sieve zeolite with defined X-ray powder diffraction pattern, as adsorbent and catalyst: Engelhard Minerals Corp; Engelhard Corp.
- [8] Rocha, J.; Anderson, M. W. Microporous titanosilicates and other novel mixed octahedral-tetrahedral framework oxides. *European Journal of Inorganic Chemistry*, n. 5, p. 801-818, May 2000.  
[https://doi.org/10.1002/\(SICI\)1099-0682\(200005\)2000:5<801::AID-EJIC801>3.0.CO;2-E](https://doi.org/10.1002/(SICI)1099-0682(200005)2000:5<801::AID-EJIC801>3.0.CO;2-E)
- [9] Rocha, J.; LIN, Z. Microporous mixed octahedral-pentahedral-tetrahedral framework silicates. *Micro- and Mesoporous Mineral Phases*, v. 57, p. 173-201, 2005 2005.  
<https://doi.org/10.2138/rmq.2005.57.6>
- [10] Chukanov, N. V.; Pekov, I. V. Heterosilicates with tetrahedral-octahedral frameworks: Mineralogical and crystal-chemical aspects. *Micro- and Mesoporous Mineral Phases*, v. 57, p. 105-143, 2005 2005.  
<https://doi.org/10.2138/rmq.2005.57.4>
- [11] Pekov, I. V.; Chukanov, N. V. Microporous framework silicate minerals with rare and transition elements: Minerogenetic aspects. *Micro- and Mesoporous Mineral Phases*, v. 57, p. 145-171, 2005 2005.  
<https://doi.org/10.2138/rmq.2005.57.5>
- [12] Lee, Dong-Keun; IHM, Son-Ki. Hydrogenation of carbon monoxide over cobalt containing zeolite catalysts. *Applied catalysis*, v. 32, p. 85-102, 1987.  
[https://doi.org/10.1016/S0166-9834\(00\)80618-1](https://doi.org/10.1016/S0166-9834(00)80618-1)
- [13] SHAMSI, Abolghasem *et al.* Zeolite-supported cobalt catalysts for the conversion of synthesis gas to hydrocarbon products. *Industrial & engineering chemistry product research and development*, v. 23, n. 4, p. 513-519, 1984.  
<https://doi.org/10.1021/i300016a001>
- [14] ROSSIN, Joseph A.; Saldarriaga, Carlos; Davis, Mark E. Synthesis of cobalt containing ZSM-5. *Zeolites*, v. 7, n. 4, p. 295-300, 1987.  
[https://doi.org/10.1016/0144-2449\(87\)90030-3](https://doi.org/10.1016/0144-2449(87)90030-3)
- [15] Martínez-Hernández, Angel; Fuentes, Gustavo A. Redistribution of cobalt species in Co-ZSM5 during operation under wet conditions in the reduction of NO<sub>x</sub> by propane. *Applied Catalysis B: Environmental*, v. 57, n. 3, p. 167-174, 2005.  
<https://doi.org/10.1016/j.apcatb.2004.10.018>
- [16] Martínez, Agustín *et al.* Fischer-Tropsch synthesis of hydrocarbons over mesoporous Co/SBA-15 catalysts: the influence of metal loading, cobalt precursor, and promoters. *Journal of Catalysis*, v. 220, n. 2, p. 486-499, 2003.  
[https://doi.org/10.1016/S0021-9517\(03\)00289-6](https://doi.org/10.1016/S0021-9517(03)00289-6)
- [17] Rogovin, Marina; Neumann, Ronny. Silicate xerogels containing cobalt as heterogeneous catalysts for the side-chain oxidation of alkyl aromatic compounds with tert-butyl hydroperoxide. *Journal of Molecular Catalysis A: Chemical*, v. 138, n. 2, p. 315-318, 1999.  
[https://doi.org/10.1016/S1381-1169\(98\)00207-6](https://doi.org/10.1016/S1381-1169(98)00207-6)
- [18] Backman, L. B. *et al.* A novel Co/SiO<sub>2</sub> catalyst for hydrogenation. *Catalysis today*, v. 43, n. 1, p. 11-19, 1998.  
[https://doi.org/10.1016/S0920-5861\(98\)00132-1](https://doi.org/10.1016/S0920-5861(98)00132-1)
- [19] JONG, Sung-Jeng; CHENG, Soofin. Reduction behavior and catalytic properties of cobalt containing ZSM-5 zeolites. *Applied Catalysis A: General*, v. 126, n. 1, p. 51-66, 1995.  
[https://doi.org/10.1016/0926-860X\(95\)00016-X](https://doi.org/10.1016/0926-860X(95)00016-X)
- [20] Weston, Simon C.; STROHMAIER, Karl G.; VROMAN, Hilda B. Molecular sieve material, its synthesis and use. U.S. Patent n. 9,452,423, 27 set. 2016.
- [21] Davis, Mark E.; TAKEWAKI, Takahiko. Molecular sieve CIT-6. U.S. Patent n. 6,521,206, 18 fev. 2003.
- [22] ROTH, Wieslaw J. *et al.* Molecular sieve composition (EMM-10), its method of making, and use for hydrocarbon conversions. U.S. Patent n. 8,529,752, 10 set. 2013.
- [23] Elomari, Saleh. Using molecular sieve SSZ-65 for reduction of oxides of nitrogen in a gas stream. U.S. Patent Application n. 10/956,276, 30 set. 2004.
- [24] C.C. Pavel, D. Vuono, I.V. Asafei, P. De Luca, N. Bilba, J.B. Nagy, A. Nastro, Study of the thermal dehydration of metal-exchange ETS-10 titanosilicate, in: J. Ćejka, N.
- [25] J.H. Choi, S.D. Kim, Y.J. Kwon, W.J. Kim, Adsorption behaviors of ETS-10 and its variant, ETAS-10 on the removal of heavy metals, Cu<sup>2+</sup>, Co<sup>2+</sup>, Mn<sup>2+</sup> and Zn<sup>2+</sup> from a wastewater, *Micropor. Mesopor. Mat.* 96 (2006) 157-167.  
<https://doi.org/10.1016/j.micromeso.2006.03.050>
- [26] Z. Lin, J. Rocha, P. Brandão, A. Ferreira, A.P. Esculcas, J.D. Pedrosa de Jesus, A. Philippou, M.W. Anderson, Synthesis and structural characterization of microporous umbite, penkviltsite, and other titanosilicates, *J. Phys. Chem. B* 101 (1997) 7114-7120.  
<https://doi.org/10.1021/jp971137n>
- [27] A.S. Paula, A. de Vasconcellos, J.A. Ellena, M. Giotto, J.G. Nery, Hydrothermal syntheses of ETS-10 like vanadosilicates using chiral organic molecules. Part I, *Microporous Mesoporous Mater.* 147 (2012) 30-46.  
<https://doi.org/10.1016/j.micromeso.2011.05.028>
- [28] F. Mani, L. Wu, S.M. Kuznicki, A simplified method to synthesize pure vanadium silicate analogue of ETS-10, *Microporous Mesoporous Mater.* 177 (2013) 91-96.  
<https://doi.org/10.1016/j.micromeso.2013.02.008>
- [29] F. Mani, J.A. Sawada, S.M. Kuznicki, Comparative adsorption study of EVS-10 and ETS-10, *Microporous Mesoporous Mater.* 204 (2015) 43-49.  
<https://doi.org/10.1016/j.micromeso.2014.10.048>
- [30] F. Mani, J.A. Sawada, S.M. Kuznicki, Spontaneous formation of silver nanoparticles on the vanadium silicate EVS-10, *Microporous Mesoporous Mater.* 224 (2016) 208-216.  
<https://doi.org/10.1016/j.micromeso.2015.11.032>
- [31] A. Altomare, C. Giacovazzo, A. Guagliardi, A. G. G. Moliterni, R. Rizzi, P. Werner, New techniques for indexing: N-TREOR in Expo, *J. Appl. Cryst.* (2000). 33, 1180-1186.  
<https://doi.org/10.1107/S0021889800006427>
- [32] A. Eldewik, R.F. Howe, Cobalt substitution in ETS-10, *Micropor. Mesopor. Mater.* 48 (2001) 65-71  
[https://doi.org/10.1016/S1387-1811\(01\)00331-6](https://doi.org/10.1016/S1387-1811(01)00331-6)
- [33] A. Grimaud, K. J. May, C. E. Carlton, Y.-L. Lee, M. Risch, W. T. Hong, J. Zhou and Y. Shao-Horn, *Nat. Commun.*, 2013, 4, 2439.  
<https://doi.org/10.1038/ncomms3439>
- [34] B. Zhao, L. Zhang, D. Zhen, S. Yoo, Y. Ding, D. Chen, Y. Chen, Q. Zhang, B. Doyle, X. Xiong and M. Liu, *Nat.*

- Commun., 2017, 8, 14586.  
<https://doi.org/10.1038/ncomms14586>
- [35] X. Miao, L. Wu, Y. Lin, X. Yuan, J. Zhao, W. Yan, S. Zhou and L. Shi, *Chem. Commun.*, 2019, 55, 1442-1445.  
<https://doi.org/10.1039/C8CC08817A>
- [36] Breck, D. W. *Zeolite Molecular Sieves: Structure, Chemistry and Use*. Wiley and Sons: London, 1974 (reprinted R. E. Krieger: Malabar, FL, 1984).
- [37] Chandrasekhar, S. Pramada, P. N, Kaolin-based zeolite Y, a precursor for cordierite ceramics, *Applied Clay Science*, 2004, 27, 187-198.  
<https://doi.org/10.1016/j.clay.2004.07.001>
- [38] Grimaud, A., May, K., Carlton, C. *et al.* Double perovskites as a family of highly active catalysts for oxygen evolution in alkaline solution. *Nat Commun* 4, 2439 (2013).  
<https://doi.org/10.1038/ncomms3439>
- [39] E. M. Flanigen, H. Khatami, H. Szymanski, *Molecular Sieve Zeolites-I*. (1974). 16, 201-229.  
<https://doi.org/10.1021/ba-1971-0101.ch016>

---

Received on 08-11-2022

Accepted on 20-12-2022

Published on 29-12-2022

DOI: <https://doi.org/10.31875/2410-4701.2022.09.10>

© 2022 Ratero *et al.*; Zeal Press.

This is an open access article licensed under the terms of the Creative Commons Attribution License (<http://creativecommons.org/licenses/by/4.0/>) which permits unrestricted use, distribution and reproduction in any medium, provided the work is properly cited.